

Measurement of the Higgs Cross Section and Mass with Linear Colliders

P. García-Abia

*Institut für Physik der Universität Basel, Klingelbergstrasse 82,
CH-4056-Basel, Switzerland*

W. Lohmann

DESY, Platanenallee 6, D-15738 Zeuthen, Germany

We report on the accuracy of the measurement of the total cross section of the process $e^+e^- \rightarrow ZH$ and of the Higgs boson mass that would be achieved in a linear collider operating at a centre-of-mass energy of 350 GeV, assuming an integrated luminosity of 500 fb^{-1} . For that we have exploited the recoil mass off the Z using its leptonic decays into electron and muon pairs. The Higgs mass is determined with 150 MeV accuracy, the recoil mass resolution is about 1.5 GeV and the cross section is obtained with a statistical error of 3%.

1 Introduction

An e^+e^- collider with centre-of-mass energy \sqrt{s} of a few hundred GeV is particularly well suited to discover the Higgs boson if its mass is of $\mathcal{O}(100 \text{ GeV})$. Even in the case a particle interpreted as the Higgs boson was discovered already at another accelerator like LHC a linear collider would provide an optimal scenario for identifying it as the Higgs boson predicted by the Standard Model¹. Crucial tests here are the values of the couplings to gauge bosons and fermions. A quantity which depends on the couplings to the gauge bosons is the Higgs boson production cross section in the Higgs-strahlung or fusion process. The couplings to different fermion species are accessible by the measurement of the Higgs boson branching fractions. For this the production cross section of Higgs bosons is needed.

In this letter, we present a method to measure the cross section for the production of the Higgs boson independent of its branching fractions exploiting the recoil-mass method. We take into account the detector resolutions, the efficiencies of lepton identification and the relevant background processes.

We also use this method to measure the mass of the Higgs boson. It should be noted, though, that this method is not the optimal for determining the Higgs mass and the accuracy quoted in this paper is not the final one to be expected from TESLA. Additional studies on the determination of the mass of the Higgs boson exploiting the decay $Z \rightarrow b\bar{b}$ and the exclusive Higgs decays are being performed.

2 Experimental Conditions

The study is performed for a linear collider operated at a centre-of-mass energy of 350 GeV. The assumed data statistics corresponds to an integrated luminosity of 500 fb^{-1} . The detector used in the simulation follows the proposal presented in the TESLA Conceptual Design Report².

The interaction region is surrounded by a central tracker consisting of a silicon microvertex detector as the innermost part and a time projection chamber. In the radial direction follows an electromagnetic calorimeter, a hadron calorimeter, the coils of a superconducting magnet and an instrumented iron flux return yoke. The solenoidal magnetic field is 3 Tesla. The central tracker momentum resolution is $\sigma_{p_t}/p_t = 7 \cdot 10^{-5} \cdot p_t$ (GeV) and the energy resolution of the electromagnetic calorimeter $\sigma_E/E = 10\%/\sqrt{E} + 0.6\%$, E in GeV. The polar angular coverage of the central tracker maintaining the resolution is $|\cos \theta| < 0.85$, above this range the tracking resolution degrades. The electromagnetic and hadron calorimeters cover the region $|\cos \theta| < 0.996$, maintaining the resolution over the whole angular range. The simulation of the detector is done with the program SIMDET³.

3 Method of the Measurement

In the energy range considered the dominant process for Higgs boson production in the Standard Model is $e^+e^- \rightarrow ZH$. To determine the cross section for this process, $\sigma(ZH)$, we exploit leptonic decays of the Z boson, $Z \rightarrow e^+e^-$ and $Z \rightarrow \mu^+\mu^-$. These final states exhibit a clean signature in the detector. Hence they are easily selected with selection efficiencies expected to be independent of the decay mode of the Higgs boson. Due to the excellent momentum and energy resolution the Z is well reconstructed and the recoil mass against the Z, $m_X^2 = s - 2 \cdot \sqrt{s} \cdot E_Z + m_Z^2$, is exploited to detect the Higgs boson and to measure its production cross section. Here E_Z and m_Z are the energy and the mass of the Z. Bremsstrahlung and beamstrahlung are taken into account.

3.1 Signal and Background

Events of the signal, $e^+e^- \rightarrow ZH$, are generated using the PYTHIA program⁴ for Higgs boson masses of 120, 140 and 160 GeV. The Standard Model cross sections and the expected event numbers corresponding to a luminosity of 500 fb^{-1} are given in Table 1.

For the background studies the following Monte Carlo generators are used: PYTHIA for $e^+e^- \rightarrow e^+e^-f\bar{f}$, $e^+e^- \rightarrow (Z/\gamma) \rightarrow f\bar{f}(\gamma)$, $e^+e^- \rightarrow W^+W^-$ and

$e^+e^- \rightarrow ZZ$, and EXCALIBUR⁵ for non-resonant Ze^+e^- and $Z\nu_e\bar{\nu}_e$ and for $We\nu_e$. The number of events expected in the most important background processes is given in Table 2.

Initial state bremsstrahlung is simulated with PYTHIA. Beamstrahlung is taken into account using the CIRCE program⁶. The impact of beamstrahlung on the recoil mass is illustrated in Figure 1. Beamstrahlung broadens the recoil boson mass distribution and hence is of importance for this study.

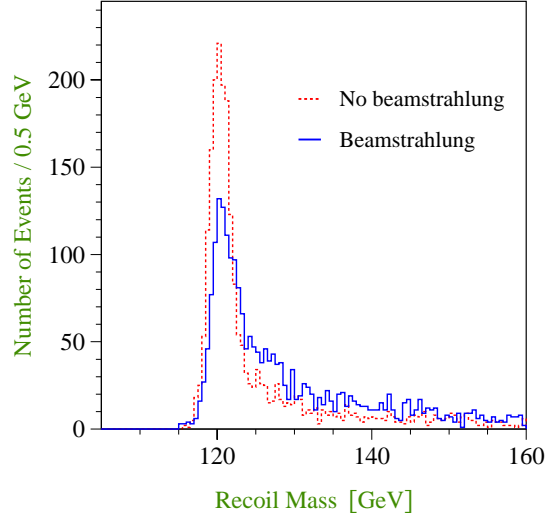


Figure 1: The recoil mass spectra off the Z with and without taking into account beamstrahlung.

Both signal and background events are processed by the detector simulation package SIMDET. The output in terms of reconstructed track momenta

m_H (GeV)	σ (fb)	events	background process	events
120	5.3	2.6×10^3	$e^+e^- \rightarrow e^+e^-ff$	2.0×10^9
140	4.3	2.1×10^3	$e^+e^- \rightarrow f\bar{f}(\gamma)$	2.0×10^7
160	3.6	1.8×10^3	$e^+e^- \rightarrow W^+W^-$	7.0×10^6
			$e^+e^- \rightarrow ZZ$	5.0×10^5

Table 1: The cross section for the process $e^+e^- \rightarrow ZH \rightarrow \ell^+\ell^-H$ for different Higgs boson masses and the number of expected events for a luminosity of 500 fb^{-1} .

Table 2: The number of events expected for several background sources.

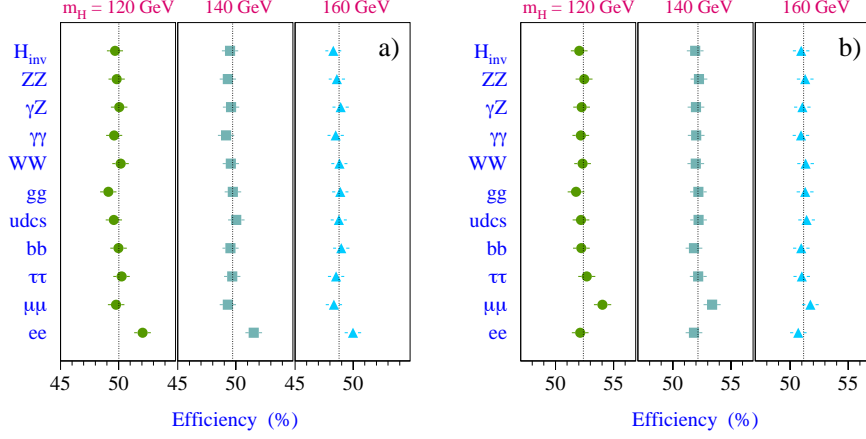


Figure 2: The selection efficiency of a) $e^+e^- \rightarrow ZH \rightarrow e^+e^-X$ and b) $\mu^+\mu^-X$ for several Higgs boson decay modes. H_{inv} stands for invisible Higgs.

and calorimetric cluster energies is used for the forthcoming analysis.

3.2 Lepton Identification and Selection of $Z \rightarrow \ell^+\ell^-$

Electrons are identified as energy deposits in the electromagnetic calorimeter whose shape is compatible with the expectation for an electromagnetic shower and with a matched track in the central tracker. The measured track momentum and shower energy must be in agreement within 5% and the shower leakage into the hadron calorimeter must be less than 2 GeV. Muons are tracks pointing to energy deposits in the calorimeters which are consistent with the expectation for a minimum ionising particle. Both electrons and muons must have momenta larger than 10 GeV and fulfil the polar angle cut $|\cos\theta| < 0.9$. The mass of the leptons is required to be within 5 GeV equal to the Z mass. To suppress background from $e^+e^- \rightarrow ZZ$, the production polar angle of the two-lepton system must be $|\cos\theta_{\ell\ell}| < 0.6$.

The selection efficiencies for the processes $e^+e^- \rightarrow ZH \rightarrow e^+e^-X$ and $\mu^+\mu^-X$ are listed in Table 3. These efficiencies are independent of the Higgs boson decay mode, as shown in Figure 2. The only exception is the case when the Higgs boson decays like the detected Z ($H \rightarrow e^+e^-$ and $H \rightarrow \mu^+\mu^-$ respectively). This modes are negligible in the Standard Model.

3.3 Results

Figure 3 shows the recoil mass distribution obtained for a $m_H = 120$ GeV signal and the background contribution for the channel $e^+e^- \rightarrow ZH \rightarrow e^+e^-X$. The Higgs boson appears well on top of a small background, mainly from $e^+e^- \rightarrow ZZ$ events.

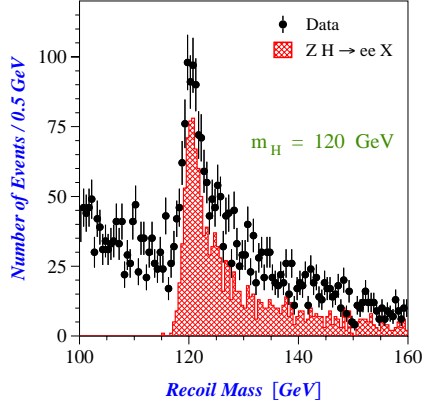


Figure 3: The recoil mass spectra off the Z in $e^+e^- \rightarrow ZH \rightarrow e^+e^-X$ events.

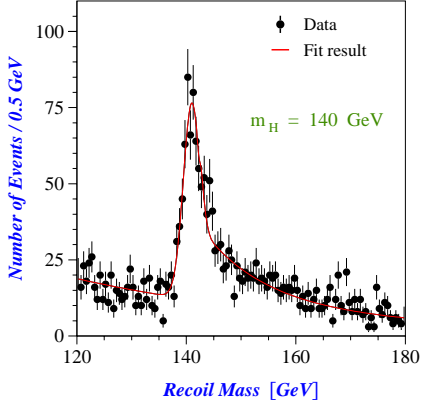


Figure 4: The fit of the recoil mass spectra off the Z in $e^+e^- \rightarrow ZH \rightarrow \mu^+\mu^-X$ events.

The recoil mass spectra are fitted with a superposition of a signal and a background distribution. To account for the asymmetric signal shape two approaches are used. One describes the left side of the signal as a Gaussian and the right side as the sum of a Gaussian and an exponential function. The other uses an Edgeworth expansion⁷ of a Gaussian. The background shape is parametrised as an exponential.

A binned χ^2 fit is performed with the mass (m_X), the width (σ_X) and the normalisation of the signal as free parameters. A typical result for the channel $e^+e^- \rightarrow ZH \rightarrow \mu^+\mu^-X$ is shown in Figure 4 for a sample generated with a Higgs boson mass $m_H = 140$ GeV.

The masses m_X agree well with the values used in the signal generation.

m_H (GeV)	e^+e^- efficiency	$H\mu^+\mu^-$ efficiency
120	50.4 ± 1.0	52.8 ± 1.0
140	49.4 ± 1.0	51.7 ± 1.0
160	48.8 ± 1.0	51.3 ± 1.0

Table 3: The selection efficiencies for $e^+e^- \rightarrow ZH \rightarrow \ell^+\ell^-X$ processes for several Higgs boson masses.

The accuracy of the mass determination is about 150 MeV, almost independent of the mass of the Higgs. The width of the distribution, reflecting the recoil mass resolution, is about 1.5 GeV. We emphasise that this method is not the optimal for determining the Higgs mass and the accuracy quoted here is not the final one to be expected from TESLA. A more accurate determination of the mass of the Higgs boson will be achieved by exploiting the decay $Z \rightarrow b\bar{b}$ and the exclusive Higgs decays.

Combining the two final states $e^+e^- \rightarrow ZH \rightarrow e^+e^-X$ and $\mu^+\mu^-X$ the cross sections are obtained with a statistical error of 2.6% to 3.1% for Higgs masses from 120 to 160 GeV. The values obtained for the production cross sections are given in Table 4, where the first error is statistical and the second is systematic.

m_H (GeV)	σ (fb) $Z \rightarrow e^+e^-$	σ (fb) $Z \rightarrow \mu^+\mu^-$
120	$5.26 \pm 0.18 \pm 0.13$	$5.35 \pm 0.21 \pm 0.13$
140	$4.38 \pm 0.18 \pm 0.11$	$4.39 \pm 0.17 \pm 0.10$
160	$3.68 \pm 0.17 \pm 0.09$	$3.52 \pm 0.15 \pm 0.08$

Table 4: The fit results for the Higgs boson production cross section. The first error is statistical and the second is systematic.

The systematic error includes the uncertainties from the selection efficiencies and a luminosity measurement error of one 1%. The former is given by the Monte Carlo statistics and can be significantly reduced. The latter dominates the total systematic error and depends on the collider parameters. Lepton misidentification, cross efficiency between decay channels and detector calibration give a negligible contribution to the systematic error.

References

1. S.L. Glashow, *Nucl. Phys.* **22**, 579 (1961);
S. Weinberg, *Phys. Rev. Lett.* **19**, 1264 (1967);
A. Salam, “Weak and Electromagnetic Interactions”, in *Elementary Particle Theory*, edited by N. Svartholm, page 367, Stockholm, 1969, Almqvist and Wiksell.
2. “Conceptual Design of a 500 GeV e^+e^- Linear Collider with Integrated X-ray Laser Facility”, Vol. I, editors R. Brinkmann, G. Materlik, J. Rossbach, A. Wagner, DESY 1997-048, ECFA 1997-182.
3. SIMDET V3.1, M. Pohl and H.J. Schreiber, DESY-99-030 (1999).
4. PYTHIA V6.115, T. Sjöstrand, *Comp. Phys. Comm.* 82 (1994) 74.
5. R. Kleiss and R. Pittau, *Comp. Phys. Comm.* 85 (1995) 447;

- R. Pittau, Phys. Lett. B 335 (1994) 490.
6. T. Ohl, The CIRCE program (V6), IKDA 96/13-rev (1996), hep-ph/9607454-rev;
H. Anlauf, IKDA 96/6 (1996), hep-ph/9602397.
 7. F.Y. Edgeworth, Trans. Cambridge Phil. Soc. 20 (1905) 36.